Journal of Energy Storage 5 (2016) 25–32

Contents lists available at ScienceDirect

Journal of Energy Storage

journal homepage: www.elsevier.com/locate/est

Experimental studies for the cyclability of salt hydrates for thermochemical heat storage

P.A.J. Donkers [a,c], L. Pel [a,*], O.C.G. Adan [a,b]

[a] Technical University Eindhoven, Den Dolech 2, 5600 MB Eindhoven, The Netherlands
[b] TNO, PO Box 49, 2600 AA Delft, The Netherlands
[c] Materials innovation institute (M2i), Elektronicaweg 25, 2628 XG Delft, The Netherlands

ARTICLE INFO

Article history:
Received 18 August 2015
Received in revised form 4 November 2015
Accepted 8 November 2015
Available online

Keywords:
Hydrates
NMR
Cyclability

ABSTRACT

Salt hydrates have promising potential as heat storage materials by use of their hydration/dehydration reaction. These hydration/dehydration reactions are studied in this paper for $CuCl_2$, $CuSO_4$, $MgCl_2$ and $MgSO_4$. During a hydration/dehydration reaction, the salt shrinks and expands as a result of the differences in densities of the phases. As a result, after the first dehydration cycle, the crystal is fractured into a pseudomorphic state that releases the water molecules more easily. The effect of fracturing is larger in case of hydrates with larger volumetric changes. In this study the performance of hydrates during cyclic loading is related to the pore water production and volume variations. On the basis of such data, it is concluded that $CuCl_2$ is the most promising heat storage material.

1. Introduction

Currently society is transitioning, from a carbon based economy to a renewable one. To transform the domestic heat demand from carbon consumption to renewable energy, various techniques are developed to generate heat like solar collectors, parabolic solar collectors, solar ponds and solar concentrators. One of the major drawbacks of these techniques is of course that sunlight is needed for the process. This makes the production of heat uncertain overtime, which could be solved by heat storage. A storage option with a promising potential is thermochemical heat storage utilizing salt hydrates, by which heat can be stored almost loss-free over long time. Several papers have been written about requirements to consider when choosing a thermochemical heat storage material [1–5].

The publication of Goldstein [6] marks the beginning of the renewed interest in these hydrates as heat storage materials. Salt hydrates can include water in a newly formed crystal structure by which chemical energy can be stored. The basic reaction behind this process can be represented as:

$$A{\cdot}xH_2O(s) \rightleftharpoons A(s) + xH_2O(g), \quad \Delta H, \tag{1}$$

wherein $A{\cdot}xH_2O$ is a solid salt complex produced from solid A and solvent H_2O. The amount of mol water inside product A is called the loading of the salt. For the decomposition of $A{\cdot}xH_2O$ energy (ΔH) has to be added, where as in the formation of $A{\cdot}xH_2O$ the same reaction energy (ΔH) is produced. While Eq. (1) is an equilibrium reaction, the state of the system can be modified by the vapor pressure and temperature of the system. This study focusses on hydrates, which (partially) dehydrate at temperatures below 150 °C.

Previous studies focussed on a single hydration or dehydration step either induced by temperature changes, i.e. using thermal gravimetric analysis (TGA) [7–9], differential scanning calorimetry (DSC) [10–12], XRD [10,13], Raman [14] and neutron diffraction [15] or by vapor pressure; i.e. using gravimetric analysis [16,17] and Raman [18–20]. Reviews on the selection of hydrates that are suitable for heat storage [5,21–23] are mainly based on single dehydration or hydration steps or are based purely on theoretical energy densities and dehydration temperatures. This selection procedure is insufficient, as it does not take account of multicyclic stability. It has been observed that the salt grains are not stable (physically, mechanically and/or chemically) over several cycles of repeated hydration and dehydration, e.g., considering changes in the rehydration/dehydration rates and/or grain sizes [24–27]. For example, during dehydration a pseudomorphic structure may appear [28,29] due to volume changes, which facilitates vapor transport through the crystal, thereby influencing the transport in time [25]. Such observations are mainly based on mass measurements and information on the crystal structure or water transport inside the grains is missing. Furthermore, a drawback of most of the techniques used in these studies is that during the dehydration

* Corresponding author.
E-mail address: l.pel@tue.nl (L. Pel).

http://dx.doi.org/10.1016/j.est.2015.11.005

Nomenclature

RH	relative humidity (%)
RH_{del}	deliquescence RH (%)
RH_{deh}	dehydration RH (%)
T	temperature (°C)
ΔH	reaction enthalpy (kJ/mol)
S	NMR signal intensity (a.u.)
t	time after excitation (s)
T_2	transversal relaxation time (s)
T_1	spin-lattice relaxation time (s)
ρ	water density (mol/m^3)

or rehydration the moist air supply is from one side of the sample only, i.e. single-sided induced hydration/dehydration. As a result most experiments are performed on sample mass below 10 mg, because in larger samples diffusion of air through the bed of grains limits the dehydration and (re)hydration processes.

In this paper, the cyclability of several hydrates is studied, which were selected on the basis of their theoretical volume variation during a hydration/dehydration reaction. Using Nuclear Magnetic Resonance (NMR), the water transport in these hydrates is studied in larger beds of grains where the moist air is blown through the bed itself. This is in contrast with techniques like TGA or DSC, where moist air can only be blown along the top of the sample. In such experiments, the number of layers of grains will affect the dehydration process as a result of vapor diffusion through the bed of grains. In the NMR experiments, this effect can be avoided as long as the moist air flow through the bed is high compared to the vapor production or consumption of the grains in the bed.

2. Methods

In this study, NMR is used to measure water in the hydrates non-destructively. The signal of water attenuates in a NMR experiment. In the case we can ignore the spin-lattice relaxation time T_1, i.e. when the repetition time $T_r > 4T_1$, this reads according to:

$$S(t) = \rho \exp\left(-\frac{t}{T_2}\right), \tag{2}$$

wherein ρ is the water density, t is the time after excitation and T_2 is the transversal relaxation time. Hence, it is possible to link the signal intensity of the NMR to the total amount of water present. In general, as to minimize the influence of T_2, the time t is chosen as short as possible. The transversal relaxation time T_2 can be related to the mobility of the proton [30,31], whereby the T_2 increases with increasing mobility.

In a sample, not all water molecules will have the same mobility and Eq. (2) can be rewritten as:

$$S(t) = \sum_i \rho_i \left(\exp\left(-\frac{t}{T_{2,i}}\right)\right) \tag{3}$$

Here i indicates the types of water in a material, ρ_i is the water density of type water i and $T_{2,i}$ the transversal relaxation time of water i. This equation therefore shows that a multi-exponential decay curve is generally observed, which is a result of different types of water with different mobility in a sample.

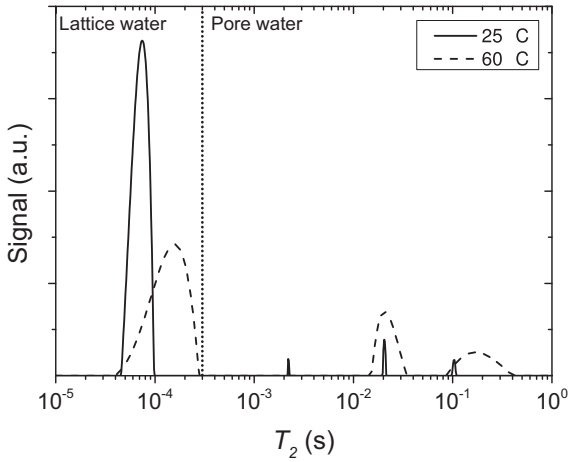

Fig. 1. The T_2 distribution of $MgSO_4{\cdot}7H_2O$ crystal before dehydration at 25 °C and during a dehydration at 60 °C. The dotted line indicates the boundary between relaxation times belonging to lattice and pore water.

In this paper, two groups of transversal relaxation times (T_2) in hydrates are considered. The first group has T_2 values between 10 and 300–1000 μs, which will be referred to as lattice water. The upper boundary is variable, depending on the studied hydrate. This type of water is located in the crystal structure and these water molecules are almost immobile and have strong static interaction with their neighboring water molecules. This component is the only component present in a hydrated crystal. As an example, in Fig. 1, the relaxation distribution is plotted for $MgSO_4$ at 25 °C and as can be seen only relaxation times below 300 μs are observed. When the sample is heated to 60 °C, the sample crosses the triple point of heptahydrate, hexahydrate and aqueous solution of $MgSO_4$ and the relaxation distribution changes. At this temperature, also T_2 values between 0.3–1 and 1000 ms are observed, which will be referred to as pore water. This water is an aqueous solution of the salt in a grain and is mobile compared to the lattice water. It may be located in voids or pores inside a grain. This water component may also appear during dehydration by crossing (incongruent) melting temperatures. In case of a larger sample, the mean relaxation time is plotted and this can be a combination of pore and lattice water.

For studying the dehydration/hydration cycles by NMR, a home-build RF-coil was used which resonates at 200 MHz, which is schematically outlined in Fig. 2. A Faraday coil has been incorporated in the RF-coil in order to be able to perform quantitative analysis of the NMR signal. The heating is performed with help of heat resistors and during heating, the temperature is controlled in a range of 20–150 °C with ±1 °C in accuracy. The temperature is measured next to the sample with help of a

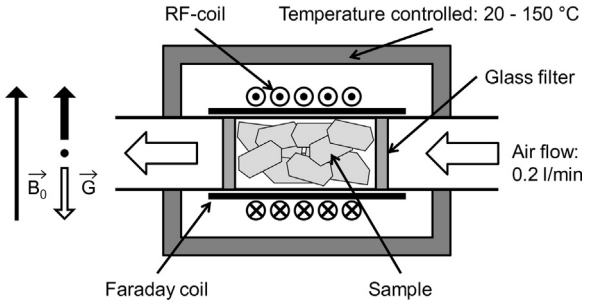

Fig. 2. A schematic representation of the NMR setup used during dehydration/hydration experiments. The sample can be conditioned by vapor pressure and temperature.

thermocouple Type K. No active cooling is present in this setup. Samples with a size of 10 mm height and 6 mm diameter (±280 mm^3) can be placed in a glass cylinder. The initial masses of the hydrated salts used in the cyclic experiments in the NMR are between 300 and 500 mg, depending on the porosity and density of the studied hydrate. The sample is confined by two porous glass filters, through which an airflow of 0.2 l/min takes place (air velocity is 11 cm/s). The airflow temperature before blowing the air into the temperature controlled setup is 25 °C. The humidity of the air was regulated by a home made humidifier and additional measured by a RH-sensor (Sensirion SHT75). All experiments were performed at atmospheric pressure. During dehydration, the air flow through the sample is kept at 0–5% RH. As the air flow first passed a glass filter, the airflow temperature which reaches the sample is equal to the temperature measured in the sample. During hydration, the RH of the air flow is set depending on the hydrate studied. The RH around the sample can be calculated with help of the initial air temperature (25 °C) and sample temperature. During our cyclic experiments we can control the temperature inside the setup and air flow through the sample.

In order to measure the relaxation, the signal decay was recorded using a CPMG pulse sequence [32]. During a CPMG pulse sequence a static magnetic field gradient of 300 mT m^{-1} is applied. This gradient adjusts the echoes of the CPMG pulse train in our recording window. The time between two successive echoes within this pulse sequence was 60 μs, whereas the repetition time of the sequence was 24 s. 1024 up to 4096 echoes were recorded, and an accumulation was performed of 4 scans during dehydration and 16 during hydration. In order to analyze the relaxation, a Fast Laplace Inversion transformation (FLI), [33], was used. The total water density was calculated based on the relaxation analysis by extrapolation of the signal to $t = 0$.

3. Materials

In this study, we have selected four hydrates based on two criteria, i.e.; firstly, the energy density calculated with the density of the hydrated salt should be in the order of 2 GJ/m^3 in the temperature range of 25–150 °C. Secondly, the crystal can be rehydrated with a difference of at least 20% RH between the applied RH and the equilibrium RH of the final loading at 25 °C. This means that at 25 °C RH_{del}–$RH_{deh} \geq 20\%$. RH_{del} is the RH where the highest loading dissolves and RH_{deh} is the RH whereby the highest loading dehydrates. Based on these criteria, four hydrates were selected: $CuCl_2$, $CuSO_4$, $MgCl_2$ and $MgSO_4$. The main thermochemical characteristics of the selected four hydrates are given in Table 1. The volume change and theoretical energy densities of the different reactions were calculated with help of Wagman et al. [34] and XRD data. The table shows that the energy density is generally larger in systems with a larger volume difference. An energy density of about 2 GJ/m^3 corresponds with a volume difference in the order of 50%.

In the experiments, grains of 1–2 mm of the chosen hydrates were used. These grains were equilibrated at 22 °C above a saturated solution of KCl (RH = 85%) for $CuSO_4$ and $MgSO_4$ salts, CH_3COOK (RH = 22%) for $MgCl_2$ and $NaNO_2$ (RH = 65%) for $CuCl_2$. With help of thermogravimetrical analysis (TGA) the initial hydrated state of the salts were determined as $CuCl_2{\cdot}2H_2O$, $CuSO_4{\cdot}5H_2O$, $MgCl_2{\cdot}6H_2O$ and $MgSO_4{\cdot}7H_2O$, which is in agreement with the expected loadings at these conditions from the phase diagrams.

4. Results

4.1. $CuCl_2$

We first studied $CuCl_2$, as this crystal can only have 2 loadings, i.e., 0 and 2. The $CuCl_2$ grains were cycled eight times in the NMR, i.e. eight times heated from 30 °C till 150 °C, with a heating rate of 0.5 °C/min. After reaching 150 °C in the sample, the temperature was kept constant for 0.5 h and decreased till 30 °C in 2 h (no active cooling, but cooling by ambient air) in each cycle. The grains were rehydrated with an RH of 60% at a sample temperature of 30 °C. The rehydration times were varied between 5 and 24 h. The resulting measured loading of the $CuCl_2$ grains as determined by NMR, as well as the measured sample temperature are plotted as a function of time in Fig. 3, whereby the time is set to zero at the start of the dehydration of each run. The first dehydration cycle shows that the crystal bed dehydrates between 80 °C and 120 °C. During the second run the bed dehydrates between 75 °C and 110 °C. The other 6 successive cycles overlap with each other and the crystals dehydrate between 70 °C and 105 °C. As can be seen the temperature of dehydration only significantly differs between the first and third dehydration run. The hydration level in all eight cycles is constant, before the dehydration starts and the crystals are entirely dehydrated at the start of the rehydration process. Within 4 h after the heating period, the sample is in a completely rehydrated phase. Moreover, the timescales for the different rehydration curves are of the same order.

As explained, with the help of NMR it is possible to determine if water is located as lattice water or pore water in a sample. In the case of $CuCl_2$ pore water was not observed on the basis of analyses of the relaxation times, both during the dehydration/hydration cycles. These experiments show that under the conditions used in this study, $CuCl_2$ is a stable material for heat storage application.

Table 1
The main thermochemical characteristics of the selected hydrates. The start loading and final loading are given in the second and third column. $\Delta_r H°$ is the standard reaction enthalpy at 25 °C and 0.1 MPa for one mol of a hydrate. ΔVolume is the volume difference between the reactors and products of the decomposition reaction. The energy density is calculated based on the reaction enthalpy and the volume of the highest hydrate in the reaction. RH_{del} is the RH where the highest loading dissolves and RH_{deh} is the RH whereby the highest loading dehydrates at 25 °C. This table is composed of data by Wagman et al. [34] and a XRD database [35].

Salt	Start loading (mol)	Final loading (mol)	$\Delta_f H°$ (kJ/mol)	ΔVolume (%)	Energy density (GJ/m^3)	RH_{del} (%)	RH_{deh} (%)
$CuCl_2$	2	0	−117.6	−43.0	1.73	70	15
$CuSO_4$	5	3	−111.70	−27.3	1.02	97	33
–	5	1	−226.55	−52.0	2.08	97	33
–	5	0	−299.20	−59.3	2.75	97	33
$MgCl_2$	6	4	−116.39	−21.6	0.90	33	3
–	6	2	−252.03	−46.6	1.95	33	3
–	6	1	−323.30	−56.8	2.49	33	3
$MgSO_4$	7	6	−59.89	−9.5	0.41	90	51
–	7	4	−166.66	−34.7	1.14	90	51
–	7	2	−283.42	−51.8	1.93	90	51
–	7	1	−335.70	−61.3	2.29	90	51
–	7	0	−411.08	−69.2	2.80	90	51

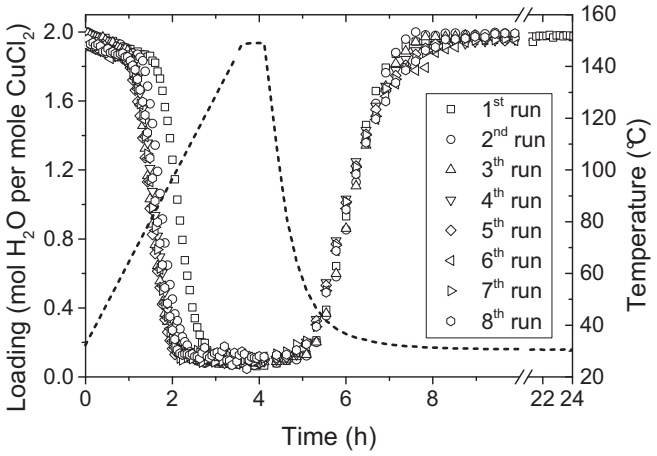

Fig. 3. The loading of a sample of $CuCl_2$ grains measured with help of NMR during different runs of dehydration/hydration. Dehydration by a heating rate of 0.5 °C/min over a temperature range of 30–150 °C, after a cooling period of 2 h (no active cooling), the sample was rehydrated with air of 30 °C and a RH of 66% over a period of 5 till 20 h. The dashed line indicates the sample temperature.

4.2. $CuSO_4$

$CuSO_4$ grains were cycled thirteen times in the NMR, whereby the dehydration was performed with a heating rate of 2 °C/min from 25 to 150 °C. After reaching 150 °C, the temperature was kept constant for 0.5 h and decreased till 25 °C in 2 h (no active cooling present) and an air flow of 25 °C and a RH of 80% was blown through the sample for 20 h. The measured loading of $CuSO_4$ grains as determined by NMR as well as the temperature are plotted as a function of time in Fig. 4, whereby the time is set to zero at the start of the dehydration of each run. The loading at the beginning of a dehydration run is decreasing with increasing number of runs, whereas the loading after dehydration was constant 0.8–1 mol water per mole $CuSO_4$ for every run. Although after the first cycle the crystal rehydrated completely, an incomplete rehydration is observed in the subsequent runs. With an increasing number of runs, the rehydration rate becomes smaller in the considered time period of 20 h.

Like for $CuCl_2$, the first run significantly differs from the other runs, i.e. the dehydration in the first run occurs at a temperature which is 20 °C higher than for the subsequent ones. The loading of the crystals for the first cycle starts to decrease strongly at 120 °C, while the other runs are almost dehydrated to an 0.8–1 mol water per mole $CuSO_4$ loading at the same temperature. Note that the loading measured in the NMR is the volume averaged water content over an entire sample, what does not imply that all mole of $CuSO_4$ have the same amount of water, i.e. local differences may occur in loading. As the measured loading of the grains is the averaged loading inside the grains this decrease of loading can be explained in two ways.

First, if we measure a loading of three water molecules per mole $CuSO_4$ in a grain (the last run), it may be interpreted as if in every grain three molecules of water surround each mole $CuSO_4$, like in the trihydrate. As dehydration of the trihydrate occurs at a higher temperature as the pentahydrate, we expect to see a shift of the dehydration process to higher temperatures. Second, the measured lower loading can also be interpreted that only part of a grain is active. To reach a loading of three, in the active part of the grain (50% of the $CuSO_4$ molecules in the grain) the $CuSO_4$ molecules are surrounded by five water molecules, and that in the inactive part (50% of the $CuSO_4$ molecules in the grain) of the $CuSO_4$ molecules are only surrounded by one water molecule. In this case, the start of the dehydration will be the same as for a $CuSO_4{\cdot}5H_2O$ crystal. In case a mixture of pentahydrate and trihydrate was available in these grains, the dehydration curve will start at the same temperature as for a $CuSO_4{\cdot}5H_2O$ crystal, but the curvature would get two distinguish drops, one for the grains with pentahydrate loading and the second for grains with trihydrate loadings. These two curves can overlap with samples wherein the trihydrate grains have only a small contribution, but especially in case of higher number of runs, we should be able to distinguish the two dehydration processes.

To determine, which of both explanations holds for $CuSO_4$, we normalized the measured loading between the loading before dehydration and after dehydration for every single run and plotted the normalized loading against temperature in Fig. 5. With increasing number of runs, the dehydration is only significantly shifted to a lower temperature between the first and second run. In between the other runs, no shift is observed and the curves overlap. This indicates that the second explanation is more probable, so the active part of a grain decreases by increasing number of runs, but that this active part still hydrate to the same loading.

A T_2 relaxation analysis was also performed on the relaxation data of the NMR during rehydration at 25 °C. In the relaxation

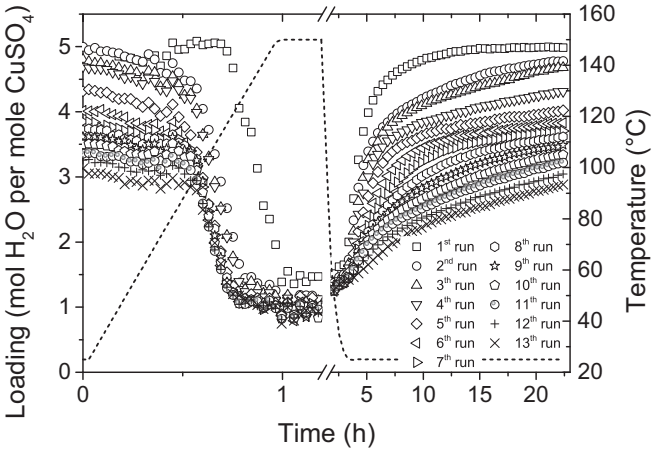

Fig. 4. The loading of a sample of $CuSO_4$ grains measured with help of NMR during different runs of dehydration/hydration. Dehydration by a heating rate of 2 °C/min over a temperature range of 25–150 °C, after a cooling period of 2 h (no active cooling), the sample was rehydrated with air of 25 °C and a RH of 80% over a period of 22 h. The dashed line indicates the sample temperature.

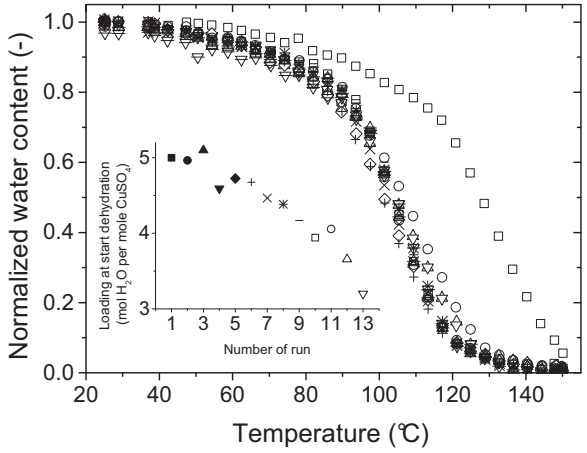

Fig. 5. The water content normalized between the maximum and minimum loading of a sample of $CuSO_4$ grains during different runs of dehydration/hydration measured with help of NMR. Dehydration by a heating rate of 2 °C/min over a temperature range of 25–150 °C (see Fig. 4). The inset gives the loading of a sample at the start of a dehydration run.

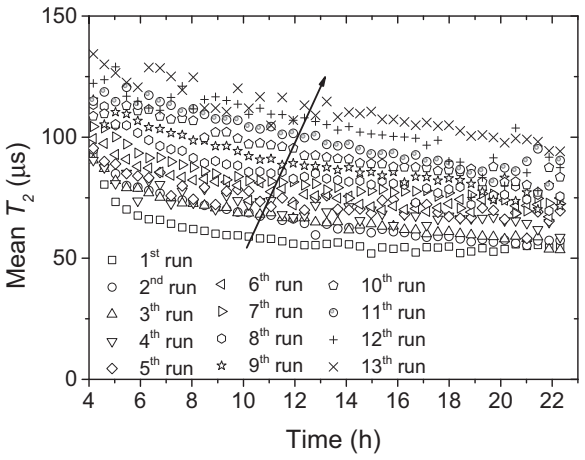

Fig. 6. The mean T_2 relaxation time of $CuSO_4$ grains during rehydration measured with help of NMR plotted against time after the start of each dehydration run with an air flow of 25 °C with a RH of 80%.

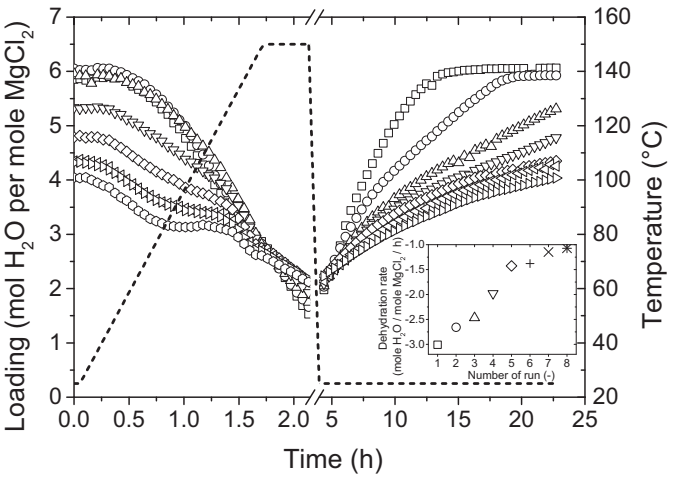

Fig. 7. The loading of a sample of $MgCl_2$ grains during different runs of dehydration/hydration measured with help of NMR. Dehydration by a heating rate of 1.2 °C/min over a temperature range of 25–150 °C. After a cooling period of 2 h (no active cooling), the sample was rehydrated with air of 25 °C and a RH of 25% over a period of 22 h. The dashed line indicates the sample temperature. The inset gives the dehydration rate at 150 °C for the different runs.

distributions only single peaks are observed with relaxation times below 0.3 ms, so only lattice water was observed during this experiment. Consequently the mean relaxation time in the sample is the relaxation time of the lattice water component during rehydration.

The mean relaxation time is plotted against time in Fig. 6. As can be seen, the mean relaxation time increases with increasing number of runs. The T_2 relaxation time of lattice water is mainly determined by static dipolar interaction of the surroundings. In case the interactions increase, the relaxation time will decrease. Hence, according to the relaxation measurement, the grains become less ordered with increasing number of runs, decreasing the interactions between the water molecules and their surroundings.

These experiments indicate that structure variations play a role in the hydration/dehydration processes. Previous experiments on sulphate hydrates have shown that the dehydration of a crystal can form a pseudomorphic structure [28,36]. The crystal will be fractured after the first dehydration run and the hypothesis we previously postulated is that during a dehydration run the crystals will form a fractured structure. As a result, in every subsequent cycle, more internal surface is available in the grains and water molecules will be adsorbed more efficiently at the outer layer of the grains. At the moment, this outer layer is completely hydrated the water pathways will be sealed off, because the outer layer will expand as result of hydration. As only a limited time is given for rehydration, this mechanism decreases the absorption rate, which will result in an incomplete rehydration. This experiment shows that $CuSO_4$ is not stable during hydration/dehydration experiments.

4.3. $MgCl_2$

For studying the dehydration and rehydration of $MgCl_2{\cdot}6H_2O$ with help of the NMR, we selected two maximum dehydration temperatures, one of 100 °C and the other one of 150 °C, resulting in a loading of respectively 4 and 2. With these two dehydration temperatures, we vary the volume change (approximately with a factor of 2) during the hydration and dehydration process and the number of phase transitions during a hydration/dehydration process.

The temperature increase to a temperature of 150 °C was performed to dehydrate the hexahydrate to dihydrate. The cycle consisted of heating of 105 min from 25 to 150 °C (i.e. 1.2 °C/min), followed by 30 min constant temperature at 150 °C. The sample was cooled down till 25 °C in 2 h (no active cooling present) and the conditions kept constant afterwards for 18 h at a RH of 25% at 25 °C. This cycle was repeated seven times. The measured loading by NMR and the temperature are plotted as function of time in Fig. 7, whereby the time is set to zero at the start of the dehydration of each run. Initially, on average the crystals dehydrate below the dihydrate phase of $MgCl_2$, but after four cycles the sample is on average dehydrated till the dihydrate. The rehydration level decreases by additional runs as result of a decreasing rehydration rate. No significant difference is observed in dehydration temperature between the first and other runs, in contrast to what we observed for $CuCl_2$ and $CuSO_4$. Moreover, dehydration still continues during the period of a constant temperature of 150 °C.

In the inset, the dehydration rate at 150 °C is plotted against the number of the run. The dehydration rate is calculated by taking the derivative in time of the loading at 150 °C. We chose 150 °C, because the temperature is constant over 30 min and the grains can only dehydrate considering that no phase transition line is crossed. In addition, during dehydration to 150 °C, the measured loading at the beginning of the 150 °C dehydration period is constant over the different runs (maximum variation of 0.25 mol H_2O per mole $MgCl_2$). The dehydration rate is smaller in case of a higher number of run. The difference may be a result of the change in grain structure, because the other conditions (temperature and air flow) are the same. Obviously, such change in grain structure decreases the releasing rate of vapor from the grain. This change in grain structure will not only affect the dehydration, but also the rehydration process.

The grain structure may be affected due to production of pore water during dehydration. Therefore, T_2 relaxation time analysis on the NMR data is performed on this dehydration experiment (in Fig. 8), the mean T_2 relaxation time of the sample is plotted against time after starting the dehydration process. In this case, the relaxation time is a combination of pore and lattice water. The initial mean relaxation time is around 400 µs at 25 °C. At the beginning of the heating of the sample, the relaxation time increases to 1 ms at 60 °C, where it remains constant till 135 °C. Until this temperature is reached, a single peak is observed in the relaxation time distribution and, consequently, water in the sample is still identified as lattice water. At 135 °C, the mean T_2 relaxation time strongly increases. The measured mean relaxation time is between 10 and 100 ms. This implies that a large part of

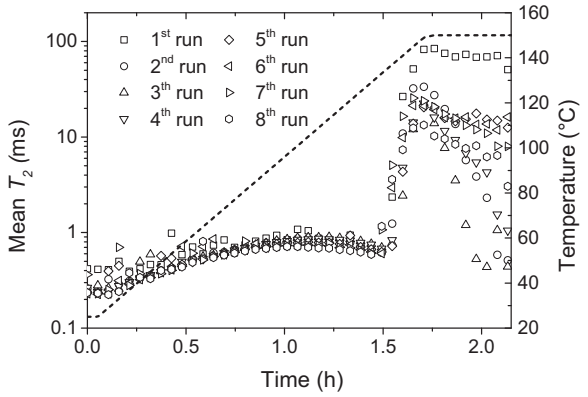

Fig. 8. The mean T_2 relaxation time of a sample of $MgCl_2$ grains measured with help of NMR plotted against time after the start of each dehydration run. The dehydration was performed with a heating rate of 1.2 °C/min. The dashed line indicates the sample temperature.

water in the crystals is pore water, i.e. mobile water in the grains. This may be explained on the basis of incongruent melting of the part of the grains at 135 °C. The transition temperature is above the triple point of heptahydrate, tetrahydrate and the solution of $MgCl_2$ [37]. So, it may happen that part of the crystal was not dehydrated till tetrahydrate and during this transition, part of the crystal is melted in its own crystal water.

The dehydration to 100 °C was performed to dehydrate the hexahydrate to tetrahydrate. The cycle consisted of a heating of 40 min from 25 to 100 °C (i.e. 2 °C/min), 50 min constant at 100 °C. The sample is cooled down till 25 °C in 2 h (no active cooling present) and the conditions are kept constant afterwards for 19.5 h at a RH of 25% at 25 °C. This cycle was repeated eleven times. The loading and the temperature are plotted against time in Fig. 9, wherein the time is set to zero at the start of the dehydration of each run. Initially crystals dehydrate below the tetrahydrate, but after four cycles the sample is, on average, dehydrated till the tetrahydrate form. The rehydration level decreases slowly by additional runs. No significant difference is observed in dehydration temperature between the first and other runs. The rehydration rate is going down with increasing number of runs, but the effect is small compared to the cycle experiment at 150 °C.

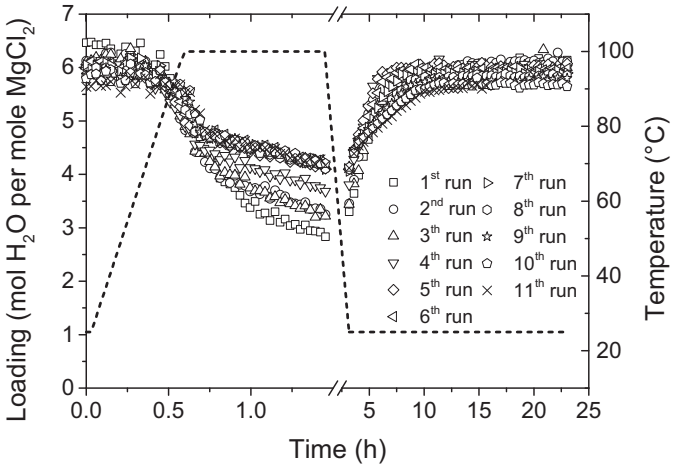

Fig. 9. The loading of a sample of $MgCl_2$ grains during different runs of dehydration/hydration measured with help of NMR. Dehydration by a heating rate of 2 °C/min over a temperature range of 25–100 °C. After a cooling period of 2 h (no active cooling), the sample was rehydrated with air of 25 °C and a RH of 25% over a period of 22 h. The dashed line indicates the sample temperature.

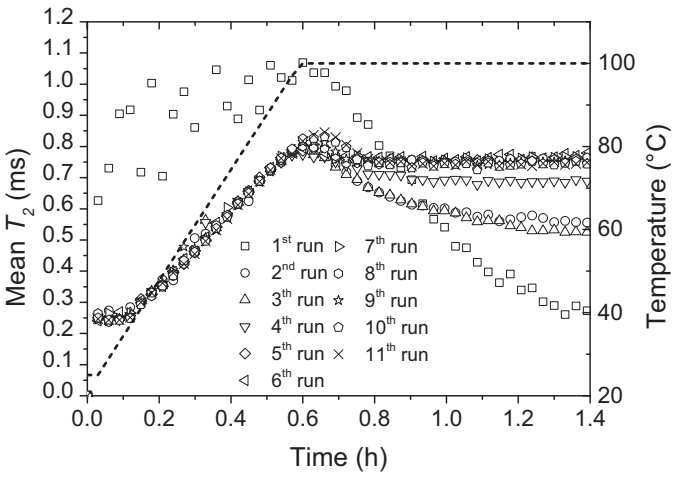

Fig. 10. The mean T_2 relaxation time of a sample of $MgCl_2$ grains measured with help of NMR plotted against time after the start of each dehydration run. The dehydration was performed with a heating rate of 2 °C/min between 25 and 100 °C. The dashed line indicates the sample temperature.

Obviously, the first four runs are different from the subsequent ones, which is also underlined in the relaxation analysis of the NMR data given in Fig. 10. In this case, the observed relaxation times are all short, indicating lattice water. In the first cycle, the mean relaxation time of the water in the sample increases during the dehydration process, and after reaching 100 °C the relaxation time decreases. In subsequent cycles, the relaxation time at temperatures below 100 °C overlap. This indicates that the water molecules in the grains experience a similar environment and have the same mobility. A difference between the runs is only visible above 100 °C, where in the runs 5–11, the relaxation time stay constant.

These two set of experiments show that $MgCl_2$ produces easily mobile water during dehydration by heating above 135 °C. This affects the grain structure, resulting in a change in the dehydration and hydration rates. A smaller dehydration step, will help to stabilize the system, but decreases at the same moment the energy storage dramatically.

4.4. $MgSO_4$

$MgSO_4$ grains were seven times cyclic loaded inside the NMR. The dehydration of $MgSO_4$ was performed with a heating rate of 0.5 °C/min from 25 to 150 °C. With the rehydration the temperature was cooled from 150 to 25 °C in 2 h and an air flow of 25 °C with 85% inflow. The loading as measured by NMR and temperature of the cyclic dehydration/hydration of $MgSO_4 \cdot 7H_2O$ is plotted as a function of time in Fig. 11, wherein the time is set to zero at the start of each dehydration run.

Obviously the maximum loading before dehydration is varying with each run (10% variations), but no clear trend downwards is observed. After dehydration, the loading is 1.2 mol H_2O per mole $MgSO_4$ for all seven runs. The first time the sample is dehydrated, the water is released at a higher temperature than in subsequent cycles. The difference in this temperature (between the first and second dehydration cycle) is about 24 °C. For the other cycles the temperature where dehydration starts slightly decreases. The rehydration rates of the first two runs are slightly lower than the other 5 runs.

The mean relaxation time and temperature are plotted as a function of time in Fig. 12. In the first run, the relaxation time is a combination of pore and lattice water. In the other runs only lattice water components are observed. We observe that the initial grains have a short relaxation time of 70 μs (1), which increases around 50 °C to 70 ms (2). This strong increase of relaxation time during

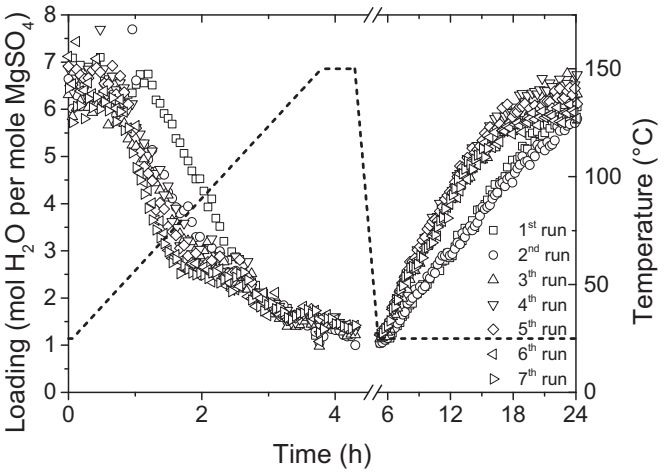

Fig. 11. The loading of a sample of $MgSO_4$ grains during different runs of dehydration/hydration measured with help of NMR. Dehydration by a heating rate of 0.5 °C/min over a temperature range of 25–150 °C, after a cooling period of 2 h (no active cooling), the sample was rehydrated with air of 25 °C and a RH of 85% over a period of 22 h. The dashed line indicates the sample temperature.

the first run indicates pore water is formed inside the grains. Such pore water formation appears after passing the triple point of heptahydrate, hexahydrate and aqueous solution of $MgSO_4$ at 48 °C. The pore water disappears at 95 °C and the relaxation time decreases to 120 μs. After 3 h of dehydration, the relaxation time increases to 250 μs (3). This is probably a result of the formation of lower hydrates, what changes the surrounding of the remaining water molecules in the crystal structure. Such production of pore water is however, not observed in the subsequent runs. During the rehydration, the mean relaxation time decreases to 120 μs, but does not drop to reach its initial value of 70 μs. The subsequent cycles overlap.

This experiment showed that during cyclic experiments with $MgSO_4$ the dehydration/hydration process is changing. The rehydration level slowly drops with increasing number of runs. With our NMR experiments we could not determine the crystal structure of $MgSO_4$, so we could not conclude anything about the influence of the known metastable phases on the cyclic dehydration/hydration process [38].

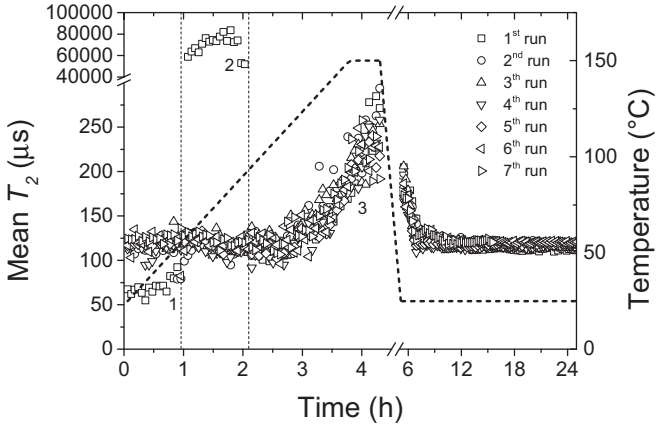

Fig. 12. The mean T_2 relaxation time of a sample of $MgSO_4$ grains measured with help of NMR plotted against time after the start of each dehydration run. The dehydration was performed with a heating rate of 0.5 °C/min between 25 and 150 °C, after a cooling period of 2 h (no active cooling), the rehydration was performed with an air flow of 25 °C with a RH of 85%. The dashed line indicates the sample temperature.

5. Discussion and conclusion

A relative hydration level of the considered salts was defined on the basis of the ratio of the loading at the start of each dehydration run and the initial loading of the sample. This relative hydration level is plotted against increasing number of runs in Fig. 13 for all salts studied. Obviously, the level of relative hydration level is constant for $CuCl_2$ and $MgCl_2$ (100 °C) grains rehydrate up to 90% for the first 11 runs. The decrease in relative hydration level is larger for the other three dehydration/hydration reactions. The hydration level of $MgSO_4$ strongly fluctuates over the measured runs between 95 and 85% and shows a decreasing hydration level with increasing number of cycles. Both $CuSO_4$ and $MgCl_2$ (150 °C) show a decreasing trend in dehydration after the first three runs.

The production of pore water measured with NMR may probably be considered as a good indicator with respect to the potential to return to the initial loading. This is exemplified in the dehydration/hydration reaction of $MgCl_2$ at 100 °C and 150 °C. In case no pore water is produced, i.e. at 100 °C, the performance in terms of recuperation of the original loading only slightly changes with increasing number of runs. In case pore water is produced, the hydration level decreases steeply (i.e. consider the 150 °C run).

Considering the four reactions without pore water production, the theoretical volume variations in $CuCl_2$ and $MgCl_2$ (100 °C) are smallest, i.e. 43.0% and 21.6%, respectively. The other two reactions have larger theoretical variations of 52.0% and 61.3% for $CuSO_4$ and $MgSO_4$, respectively. This set of experiments indicates that volume variations between a hydrate and dehydrate may be related to the stability of a dehydration/hydration reaction. As we did not measure the volume variations or the crystal structures during hydration/dehydration runs we cannot draw solid conclusions about the stability of the loading with respect to the volume variations. Besides the crystal structure variations inside a grain, also the structure of the granular bed can change during hydrations as the grains agglomerate if the applied RH is above the RH_{del}, that can have its affects on the hydration or dehydration rate. In further research attention should be drawn to these kinds of variations, with help of X-ray computed tomography (CT-scan) for variations in a granular bed and XRD for crystal structure changes.

Grains that are dehydrated for the first time (original grains) obviously dehydrate at higher temperatures than grains that dehydrate in subsequent runs. This may be a result of the vapor mobility in a grain. In an original grain the mobility is low, as the evaporation of the vapor only takes place at the walls of the grains. In case the grain is dehydrated, the grain is fractured in a pseudomorphic structure [28,36]. This pseudomorphic structure adsorbs and

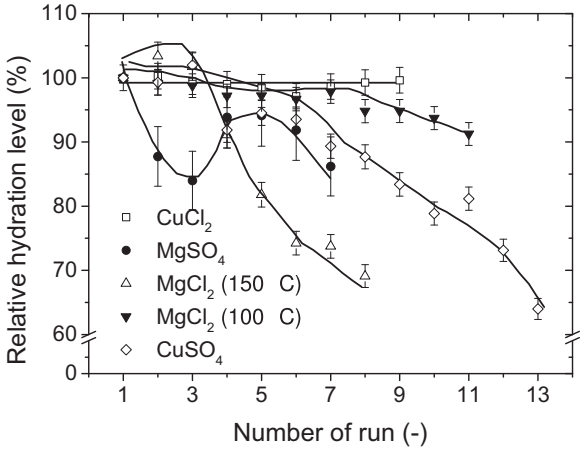

Fig. 13. The relative hydration level at the beginning of each hydration/dehydration run measured with help of NMR is plotted against the number of the run.

desorbs water faster than the original crystal, because more surface is available and paths reach the outer surface. A difference is observed of 10 °C for $CuCl_2$, 20 °C for $CuSO_4$ and 24 °C for $MgSO_4$.

These experiments show $CuCl_2$ to be the most promising heat storage material based on used conditions of these cycling tests to store heat from the point of view of stability, and considering the experimental conditions applied, with this limited number of runs. It has a constant rehydration level and reaches a heat storage capacity of 1.2 GJ/m^3 with a porosity of 30%. $MgCl_2$, $MgSO_4$ and $CuSO_4$ have higher theoretical storage potentials (about ±20% higher), but this energy storage density appears not fully available in cyclic hydration/dehydration as result of incomplete rehydration.

Acknowledgment

This research was carried out under the project number M75.7.11421 in the framework of the Research Program of the Materials innovation institute (M2i) (www.m2i.nl) supported by TNO.

References

[1] A. Solé, X. Fontanet, C. Barreneche, A.I. Fernández, I. Martorell, L.F. Cabeza, Requirements to consider when choosing a thermochemical material for solar energy storage, Sol. Energy 97 (2013) 398–404.
[2] H. Lahmidi, S. Mauran, V. Goetz, Definition, test and simulation of a thermochemical storage process adapted to solar thermal systems, Sol. Energy 80 (7) (2006) 883–893.
[3] C. Bales, Thermal properties of materials for thermo-chemical storage of solar heat, in: Tech. rep., Report of IEA Solar Heating and Cooling Programme – Task 32 "Advanced storage concepts for solar and low energy buildings", 2005.
[4] J. Cot-Gores, A. Castell, L. Cabeza, Thermochemical energy storage and conversion: a-state-of-the-art review of the experimental research under practical conditions, Renew. Sustain. Energy Rev. 16 (2012) 5207–5224.
[5] K. N'Tsoukpoe, T. Schmidt, H. Rammelberg, B. Watts, W. Ruck, A systematic multi-step screening of numerous salt hydrates for low temperature thermochemical energy storage, Appl. Energy 124 (2014) 1–16.
[6] M. Goldstein, Some physical chemical aspects of heat storage, in: UN Conf. New Sources Energy, Rome, vol. 3, 1961, 411–417.
[7] H. Zondag, V. Essen van, M. Bakker, Application of $MgCl_2{\cdot}6H_2O$ for thermochemical seasonal solar heat storage, in: 5th Int. Renew. Energy, 2010, p. 8.
[8] H. Zhu, X. Gu, K. Yao, L. Gao, J. Chen, Large-scale synthesis of $MgCl_2{\cdot}6NH_3$ as an ammonia storage material, Ind. Eng. Chem. Res. 48 (2009) 5317–5320.
[9] J. Paulik, F. Paulik, M. Arnold, Dehydration of magnesium sulphate heptahydrate investigated by quasi isothermal-quasi isobaric TG*, Thermochim. Acta 50 (1981) 105–110.
[10] Q. Huang, G. Lu, J. Wang, J. Yu, Thermal decomposition mechanisms of $MgCl_2{\cdot}6H_2O$ and $MgCl_2{\cdot}H_2O$, J. Anal. Appl. Pyrolysis 91 (2011) 159–164.
[11] E. Bevers, P.J. van Ekeren, W. Haije, H. Oonk, Thermodynamic properties of lithium chloride ammonia complexes for application inahigh-lifthigh temperature chemical heat pump, J. Therm. Anal. Calorim. 86 (2006) 825–832.
[12] L. Guangming, Investigation of thermal decomposition of $MgCl_2$ hexammoniate and $MgCl_2$ biglycollate biammoniate by DTA-TG, XRD and chemical analysis, Thermochim. Acta 412 (2004) 149–153.
[13] C. Ferchaud, H. Zondag, J. Veldhuis, R. Boer De, Study of the reversible water vapour sorption process of $MgSO_4{\cdot}7H_2O$ and $MgCl_2{\cdot}6H_2O$ under the conditions of seasonal heat storage, in: Proc. 6th Eur. Therm. Sci. Conf, 2012, p. 10.
[14] S. Brotton, R. Kaiser, In situ Raman spectroscopic study of gypsum ($CaSO_4{\cdot}2H_2O$) and epsomite ($MgSO_4{\cdot}7H_2O$) dehydration utilizing an ultrasonic levitator, J. Phys. Chem. Lett. 4 (2013) 669–673.
[15] W. Abriel, K. Reisdorf, J. Pannetier, Dehydration reactions of gypsum: a neutron and X-ray diffraction study, J. Solid State Chem. 85 (1990) 23–30.
[16] E. Crowther, J. Coutts, A discontinuity in the dehydration of certain salt hydrates, Proc. R. Soc. A 106 (1924) 215–222.
[17] R. Ford, G. Frost, The low pressure dehydration of magnesium sulphate heptahydrate and cobaltous chloride hexahydrate, Can. J. Chem. (1956) 591–599.
[18] A. Wang, J. Freeman, B. Jolliff, Phase transition pathways of the hydrates of magnesium sulfate in the temperature range 50 °C to 5 °C: implication for sulfates on Mars, J. Geophys. Res. 114 (2009) E04010.
[19] R. Wheeler, G. Frost, A comparative study of the dehydration kinetics of several hydrated salts, Can. J. Chem. (1954) 546–561.
[20] K. Linnow, M. Niermann, D. Bonatz, K. Posern, M. Steiger, Experimental studies of the mechanism and kinetics of hydration reactions, Energy Procedia 48 (2014) 394–404.
[21] C. Bales, Final report of Subtask B "Chemical and Sorption Storage". The overview, in: Tech. rep., Report of IEA Solar Heating and Cooling Programme – Task 32 "Advanced storage concepts for solar and low energy buildings", 2008.
[22] V. Essen van, J. Gores, L. Bleijendaal, H. Zondag, R. Schuitema, W. Helden van, Characterization of salt hydrates for compact seasonal thermochemical storage, in: Proc. ASME 3rd Int. Conf. Energy Sustain., 2009, p. 8.
[23] T. Yan, R. Wang, T. Li, L. Wang, I. Fred, A review of promising candidate reactions for chemical heat storage, Renew. Sustain. Energy Rev. 43 (2015) 13–31, doi:10.1016/j.rser.2014.11.015.
[24] H. Zondag, V. Essen van, R. Schuitema, A. Kalbasenka, M. Bakker, Engineering assessment of reactor designs for thermochemical storage of solar heat, in: Effstock 2009, Therm. Energy Storage Effic. Sustain., 2009, 1–8.
[25] Y. Criado, M. Alonso, J. Abanades, Kinetics of the $CaO/Ca(OH)_2$ hydration/dehydration reaction for thermochemical energy storage applications, Ind. Eng. Chem. Res. 53 (2014) 12594–12601.
[26] R. Eckhardt, P. Fichte, T. Flanagan, Kinetics of rehydration of crystalline anhydrides. Manganous formate, Trans. Faraday Soc. 67 (1971) 1143–1154.
[27] M. Stanish, D. Perlmutter, Rate processes in cycling a reversible gas–solid reaction, AIChE J. 30 (1984) 56–62.
[28] C. Rodriguez-Navarro, E. Doehne, Salt weathering: influence of evaporation rate, supersaturation and crystallization pattern, Earth Surf. Process. Landforms 24 (1999) 191–209.
[29] J. Mutin, G. Watelle, Y. Dusausoy, Study of a lacunary solid phase l – thermodynamic crystallographic characteristics of its formation, J. Solid State Chem. 27 (1979) 407–421.
[30] M. Vlaardingerbroek, J. Den Boer, Magnetic Resonance Imaging: Theory and Practice, third ed., Springer-Verlag, 2003.
[31] N. Bloembergen, E. Purcell, R. Pound, Relaxation effects in nuclear magnetic resonance absorption, Phys. Rev. 73 (1948) 679–712.
[32] S. Meiboom, D. Gill, Modified spin-echo method for measuring nuclear relaxation times, Rev. Sci. Instrum. 29 (1958) 688–691.
[33] Y.-Q. Song, L. Venkataramanan, M. Hürlimann, M. Flaum, P. Frulla, C. Straley, T(1)–T(2) correlation spectra obtained using a fast two-dimensional Laplace inversion, J. Magn. Reson. 154 (2002) 261–268.
[34] D. Wagman, W. Evans, V. Parker, R. Schumm, I. Halow, S. Bailey, K. Churney, R. Nuttall, The NBS tables of chemical thermodynamic properties, J. Phys. Chem. Ref. Data 11 (1982) 302.
[35] D.S. Kabekkodu (Ed.), PDF-2 2001 (Database), International Centre for Diffraction Data, Newtown Square, PA, USA, 2001.
[36] J. Mutin, G. Watelle, Study of a lacunary solid phase and kinetic characteristics of its formation, J. Solid State Chem. 28 (1979) 1–12.
[37] G. Kipouros, D. Sadoway, The chemistry and electrochemistry of magnesium production, Adv. Molten Salt Chem. 6 (1987) 127–209.
[38] M. Steiger, K. Linnow, D. Ehrhardt, E. Rosenberg, Decomposition reactions of magnesium sulfate hydrates and phase equilibria in the $MgSO_4$–H_2O and Na^+–Mg^{2+}–Cl^-–SO_4^{2-}–H_2O systems with implications for Mars, Geochim. Cosmochim. Acta 75 (2011) 3600–3626.